X-ray resonant scattering study of the structural and magnetic transitions in PrB_6

H. C. Walker, K. A. McEwen,* and D. F. McMorrow
Department of Physics and Astronomy and London Centre for Nanotechnology, University College London, Gower Street, London WC1E 6BT, United Kingdom

M. Bleckmann
Institute for Physics of Condensed Matter, TU Braunschweig, 38106 Braunschweig, Germany

J.-G. Park and S. Lee†
Department of Physics and Institute of Basic Science, SungKyunKwan University, Suwon 440-746, Korea

F. Iga
Department of Quantum Matter, School of Advanced Sciences of Matter, Hiroshima University, Higashi-Hiroshima 739-8530, Japan

D. Mannix‡
XMaS beamline, European Synchrotron Radiation Facility, 38043 Grenoble, France

(Received 10 September 2008; revised manuscript received 6 January 2009; published 2 February 2009)

We have made an extensive study of PrB_6 using x-ray resonant scattering to investigate both the lattice and magnetic properties. We have identified a structural distortion associated with the incommensurate to commensurate magnetic phase transition at $T=4.5$ K. Magnetic satellite reflections have been observed in the incommensurate and commensurate phases. The azimuthal dependence of the scattered intensity from the commensurate magnetic satellite reflection at $(\frac{1}{2},\frac{5}{4},\frac{5}{4})$ is consistent with the model for the magnetic structure deduced from earlier neutron-diffraction results. Evidence for possible quadrupolar ordering is discussed.

DOI: 10.1103/PhysRevB.79.054402 PACS number(s): 75.25.+z, 75.10.−b, 75.30.Kz, 61.05.cp

I. INTRODUCTION

The RB_6 compounds have attracted significant theoretical and experimental attention in recent years as they show a variety of interesting electronic and magnetic properties, for example, mixed-valence behavior in the narrow-band gap semiconductor SmB_6,[1–3] and quadrupolar order in the dense Kondo material CeB_6.[4–6] The remaining compounds are either antiferromagnetic metals in the case of the rare-earth ion being trivalent, as for the case of PrB_6, or ferromagnetic semiconductors if the ion is divalent.[7]

The rare-earth hexaborides crystallize in the CaB_6 structure (space group $Pm\bar{3}m$), with the rare-earth ions situated at the vertices of the cubic cell containing the B_6 octahedron, and the boron ions at the $6f$ positions $(x,\frac{1}{2},\frac{1}{2})$, where $x \simeq 0.2$. This simple crystal structure makes them attractive model systems for the study of multipolar order and its role in the magnetic and electrical properties of f electron systems. For PrB_6 the lattice parameter $a=4.13$ Å. It exhibits two magnetic phase transitions: (i) at $T_{N1}=7$ K to an incommensurate (IC) antiferromagnetic (AFM) phase with ordering wave vector $\mathbf{k}_1=(\frac{1}{2},\frac{1}{4}-\delta,\frac{1}{4})$, with $\delta\approx 0.05$, and (ii) at $T_{N2}=4.5$ K to a commensurate (C) AFM phase with $\mathbf{k}_2=(\frac{1}{2},\frac{1}{4},\frac{1}{4})$.[8,9]

Early inelastic neutron-scattering (INS) measurements on paramagnetic PrB_6 revealed the crystal-field splitting of the Hund's rules $J=4$ multiplet into a Γ_5 triplet ground state with a Γ_3 doublet at 27 meV, a Γ_4 triplet at 32 meV, and a Γ_1 singlet 39 meV.[10] Such a crystal-field level scheme is consistent with the high-temperature magnetic susceptibility.[11] In the ordered phases, the ground-state triplet is split by the molecular field. A detailed INS study of the low-energy excitations in both the IC and C phases has recently been made with single-crystal PrB_6.[12] There is significant dispersion in the excitations in both phases, indicating interactions out to the fourth nearest neighbors.

Burlet *et al.*[8] interpreted their PrB_6 single-crystal neutron-diffraction results in terms of a planar $2k$ magnetic structure, see Fig. 1, that in the commensurate phase is reminiscent of the phase III structure of CeB_6.[13] This commonality suggests that the antiferromagnetic commensurate structure may coexist with an $\mathcal{O}_{xy}$-type antiferroquadrupolar order. In addition, Burlet *et al.*[8] deduced the ordered moment to be only $1.2\mu_B$/Pr ion although the earlier powder-diffraction study[9] indicated a moment of $1.77\mu_B$/Pr ion. In contrast, we expect a moment of $2.0\mu_B$/Pr ion for the Γ_5 triplet ground state. It has been postulated[11] that this discrepancy originates from the competition between antiferromagnetic and quadrupolar

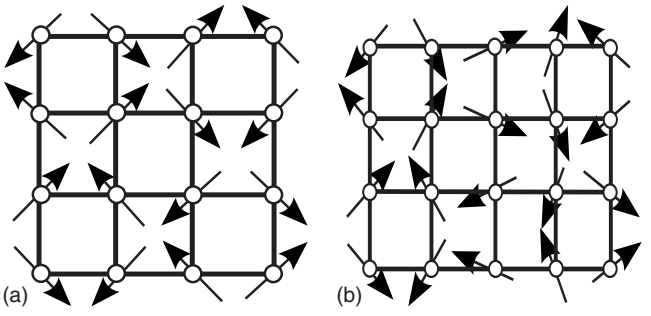

FIG. 1. The magnetic structures in the (a) commensurate and (b) incommensurate phases deduced from neutron-diffraction measurements (Ref. 8).

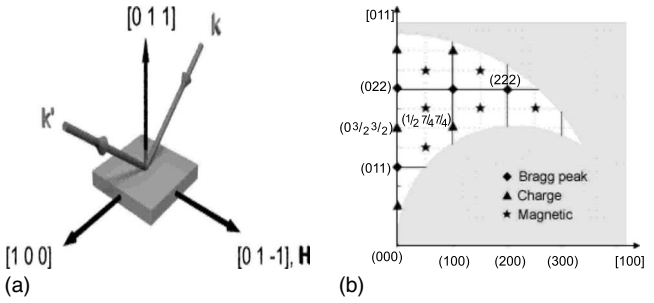

FIG. 2. (a) Schematic showing the experimental setup. (b) A map of the accessible region of reciprocal space for PrB_6 for the vertical scattering plane of the diffractometer when using x-rays with $E=6.440$ keV, corresponding to the Pr L_{II} edge.

exchange interactions and that PrB_6 might be understood as being intermediate in terms of exchange interactions between antiferroquadrupolar ordered CeB_6 with $\mathbf{k}_Q=(\frac{1}{2},\frac{1}{2},\frac{1}{2})$ and the collinear antiferromagnet NdB_6 with $\mathbf{k}_M=(0,0,\frac{1}{2})$.[14] However, as yet there has been no direct evidence of quadrupolar order, and this has motivated our study.

In this paper, we report the results of a detailed study of the magnetic ordering and a search for possible quadrupolar ordering using x-ray resonant scattering (XRS) techniques. We have discovered a structural transition that accompanies the IC-C phase transition at T_{N2}.

II. EXPERIMENTAL DETAILS

A single crystal of PrB_6 was prepared using a traveling-solvent-floating-zone method in a mirror furnace equipped with Xe lamps at Hiroshima University. The sample was cut and aligned to give a face normal to the [011] direction and polished using fine diamond paste. XRS measurements were performed on the U.K.-CRG x-ray magnetic scattering (XMaS) bending magnet beamline[15] at the European Synchrotron Radiation Facility, where wave-vector resolution is typically of the order of 1×10^{-4} Å^{-1}. A vertical scattering reflection geometry was used to give the [011]-[100] scattering plane (see Fig. 2) with the incoming beam σ polarized.

The beamline was optimized to work at the praseodymium L_{II} edge in order to probe the Pr $5d$ states at the $E1$ dipolar resonance and the $4f$ states at the $E2$ quadrupolar resonance. To enable polarization analysis of the diffracted beam, we employed a copper (2 2 0) crystal analyzer. However, this was not at the ideal analyzer Bragg angle of $2\theta=90°$. Such an angle would correspond to an x-ray energy of 6.860 keV, some 400 eV away from the L_{II}-edge energy of 6.440 keV at which we operated. The departure from the ideal angle of $\theta=45°$ introduces a correction to the measured intensities, with cross-talk between the $\sigma-\pi$ and $\sigma-\sigma$ channels. Nevertheless, this was the most suitable analyzer available to us, with a cross-talk of ~4% as measured on a Bragg peak. Both charge and magnetic reflections were studied, and the temperature, magnetic field, and azimuthal dependences of the scattering intensities were investigated. For azimuthal measurements, in which the scattered intensity is measured as a function of the azimuthal angle rotated about the scattering vector, the sample was mounted in a Joule-Thomson cryostat that can be operated over a wide range of angles while maintaining base temperature.

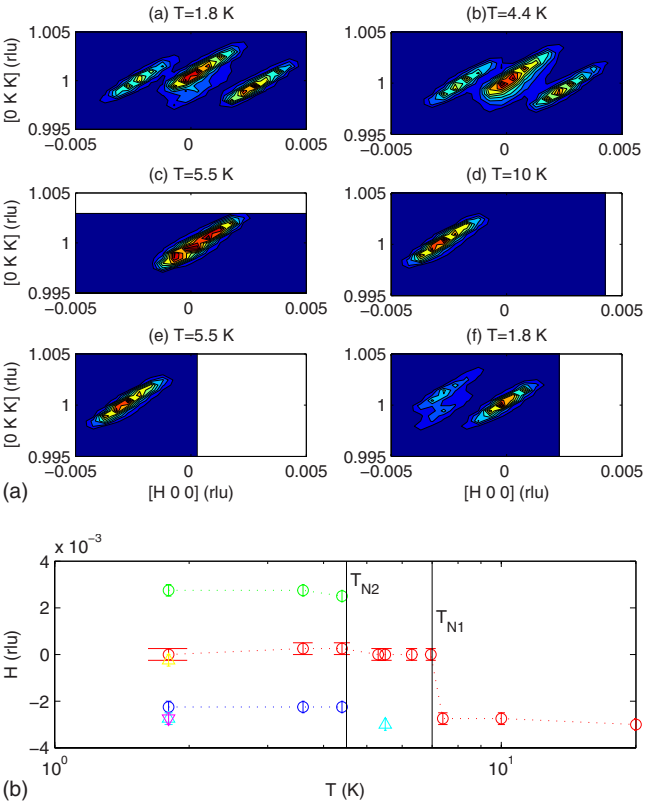

FIG. 3. (Color online) Reciprocal space mesh scans of PrB_6 near the (011) Bragg peak position at a series of temperatures measured in the sequence (a)→(f), showing multiple peaks in the low-temperature C phase, but only one peak at higher temperatures. Also shown is a figure showing the evolution of the peak positions with temperature (warming ○ and cooling △).

For magnetic-field-dependent studies, the sample was mounted in the XMaS/AMI superconducting magnet, which can deliver up to 4 T. The field was applied transverse to the x-ray beam along the $[01\bar{1}]$ direction, as shown in the schematic Fig. 2(a).

III. RESULTS AND DISCUSSION

A. Bragg peaks and structural distortion in zero field

On aligning the PrB_6 sample at base temperature (1.7 K), the specular Bragg reflection (0 1 1) in the $\sigma-\sigma$ channel showed multiple peaks in the θ rocking curve, while at 10 K only one peak was observed for the same measurement. McCarthy *et al.*[9] previously proposed a structural distortion at low temperatures but were unable to detect this in their neutron-diffraction measurements due to insufficient wave-vector resolution. To investigate this possibility, we utilized the much higher wave-vector resolution available with x-rays at XMaS. Mesh scans of reciprocal space close to (0 1 1), performed as a function of temperature, clearly revealed a small peak splitting (~0.3%) at low temperatures (see Fig. 3). At base temperature the mesh scan [Fig. 3(a)] shows at

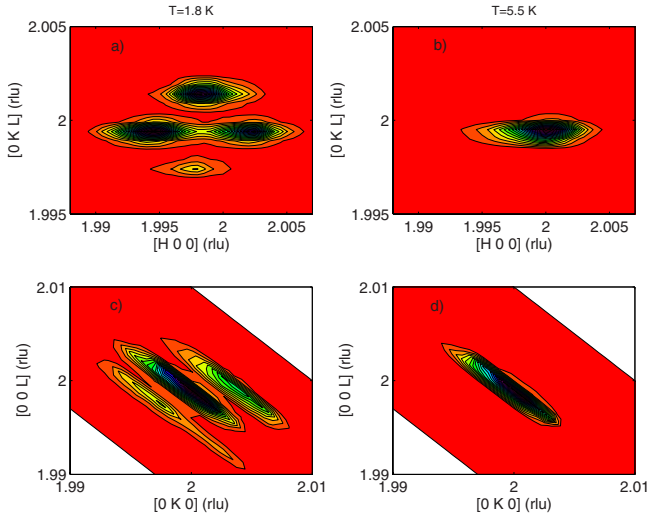

FIG. 4. (Color online) Reciprocal space mesh scans of PrB_6 around the (222) Bragg peak position: (a) in plane at $T=1.8$ K, showing four peaks, (b) the same in-plane scan performed at $T=5.5$ K with only one peak; [(c) and (d)] perpendicular cuts through the peaks at $T=1.8$ and 5.5 K, respectively, for $h=1.998$ rlu.

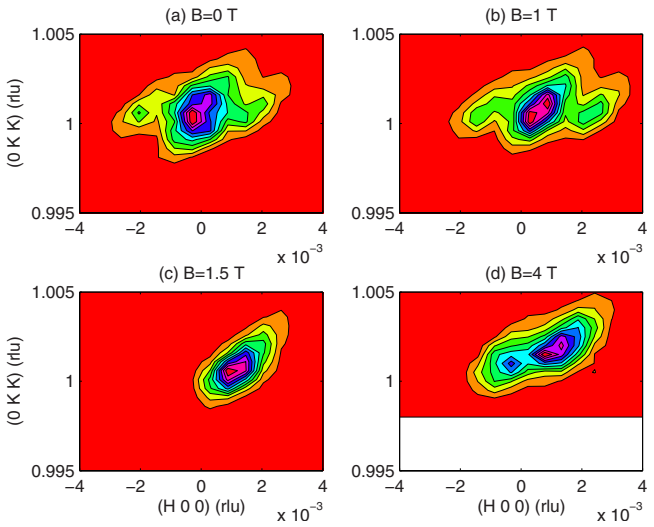

FIG. 5. (Color online) Reciprocal space mesh scans of PrB_6 around the (0 1 1) Bragg peak position at $T=2$ K in various magnetic fields applied along $[01\bar{1}]$.

least three and possibly four peaks, with the fourth peak being much weaker and very close in position to the most intense peak. These peaks were detected up to $T=4.4$ K, changing little in intensity or position, but at $T \geq 5.3$ K only one peak is observed at the position where previously there had been the greatest intensity. This observation indicates that the structural transition is associated with the C-IC magnetic transition at $T_{N2}=4.5$ K.

There is also a clear shift in the position of the single peak to more negative h for $T>7$ K, i.e., in the paramagnetic phase. It is apparent that the positions of the multiple peaks due to the structural distortion are dependent on the thermal history. As the sample was heated from $T=7-20$ K, the peak position of the single Bragg peak at (011) was unchanged. The sample was then cooled back down below T_{N1}. At $T=5.5$ K, i.e., in the incommensurate magnetic phase, the peak position is unchanged from that in the paramagnetic phase. Within the commensurate phase, splitting of the peaks is observed again, but it differs from that seen previously, and hence the thermal history was then taken into account when performing all further measurements. The most intense peak seen in the mesh, however, appears to be at the same position, cf. Figs. 3(a) and 3(f). The temperature dependence of the peaks, under warming and cooling conditions, is shown also in Fig. 3.

The splitting of a Bragg reflection into at least four peaks is seen more clearly for the (2 2 2) reflection. We performed two sets of mesh scans perpendicular to one another through reciprocal space to gain an understanding of the three-dimensional peak splitting. Figure 4 shows these mesh scans at $T=1.8$ and 5.5 K, revealing four peaks in plane at low temperature, which appear as three peaks in the perpendicular plane due to the overlap of two of the peaks. Again only one peak is observed at 5.5 K.

Based on our present data, we cannot unambiguously deduce the type of structural distortion. For example, one might assume that a tetragonal distortion, in which the length of only one axis is changed, would lead to a maximum of three peaks for the three possible domains, and therefore exclude it. However, a rotation between domains can lead to up to 15 different reciprocal lattice points.[16] The observation of the (2 2 2) Bragg peak splitting into four peaks in the commensurate phase is consistent with a rhombohedral distortion. This conclusion is in accord with that of McCarthy *et al.*[9] who suggested that quadrupolar ordering at T_{N2} might induce PrB_6 to undergo a rhombohedral crystallographic distortion. In order to elucidate the nature of the distortion, a high-resolution neutron powder-diffraction experiment has been undertaken and analysis is underway.[17]

B. Magnetic field dependence of the Bragg peaks

The magnetic field dependence of the structural distortion was investigated using mesh scans in reciprocal space of the specular (0 1 1) reflection. Figure 5 shows the evolution of the peak splitting for four different applied magnetic fields. As the field is increased to 1 T, the peaks all move to slightly larger values of HKL. This implies that the lattice shrinks in an applied magnetic field. Previously negative magnetostriction was observed along the $[01\bar{1}]$ direction, while the crystal was observed to elongate along the [011] direction, keeping the cell volume almost constant for $H\|[011]$.[11] This negative change in lattice parameter for magnetic field applied perpendicular to the lattice direction is in accord with our measurements.

In an applied field of 1.5 T there is only one reflection, implying that the distortion has been suppressed. Burlet *et al.*[8] stated that at ~2 T for $H\|[011]$ the commensurate $2k$ magnetic phase underwent a transition to a collinear single k phase with the moments aligned along the $[01\bar{1}]$ direction. This change in magnetic structure has been associated with a change in the proposed quadrupolar structure to ferro-$\mathcal{O}_{xy}$ order.[11] This could alter the nature of the structural distor-

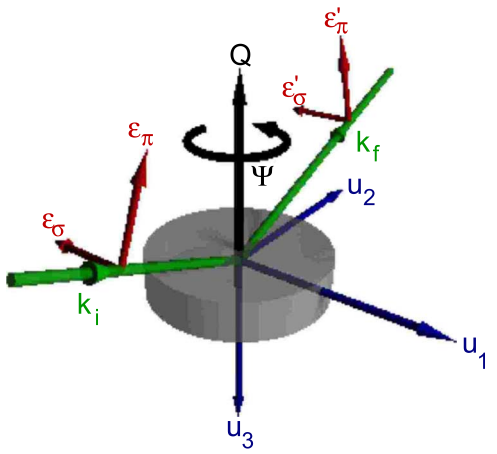

FIG. 6. (Color online) Schematic representation of the experimental setup to perform azimuthal-dependent XRS studies, where **u** are the basis vectors describing the reference frame.

tion, which might explain why at intermediate applied magnetic fields only a single peak was observed in the mesh scans. Figure 5(d) shows 4 T data, which was not collected as part of the same data set, but instead after various other peaks had been investigated. However, the temperature had not changed so there should be no problem with the thermal history, but this subplot appears to show a slightly modified splitting of the specular reflection again in this field, the origin of which is as yet undetermined.

C. Magnetic structures of PrB_6

Historically magnetic structures have usually been determined using neutron diffraction, relying on the interaction with the neutron's magnetic moment. However, as part of the electromagnetic spectrum, x-rays are also sensitive to magnetic distributions although the weak coupling results in an intensity ratio for magnetic to charge scattering of ~0.01%, making experiments very challenging. This problem is resolved by XRS techniques, which take advantage of the large enhancements of x-ray magnetic scattering signals on tuning through the absorption edge of the element being studied. Resonant behavior occurs when the incident photon energy is equal to the difference between the ground state and an intermediate state, thus probing the intermediate atomic states directly, providing sensitivity to the magnetization of *d* and *f* bands or their splitting due to multipolar interactions. In addition XRS is sensitive to higher-order multipolar order, such as quadrupolar order which cannot be studied directly using neutrons. It is a powerful tool for elucidating complex quadrupolar order as illustrated by our studies of UPd_3.[18,19]

In a radiative transition a photon is emitted with angular momentum $J=1$. The radiation field will be the sum of electric and magnetic multipolar contributions. Quantum-mechanical selection rules for the transition require that total angular momentum and parity are conserved. The transition rate decreases by a factor of $\sim 10^3$ through successive higher-order multipolar transitions, such that the electric dipole ($E1$) transition dominates. However, in several systems electric quadrupole ($E2$) transitions are also significant, e.g., DyB_2C_2.[20] At the Pr L_{II} edge the $E1$ transition connects $2p_{1/2} \rightarrow 5d$ states, while the $E2$ transition connects to the lower-energy $4f$ states.

The x-ray resonant magnetic scattering (XRMS) electric dipole ($E1$) amplitude has been formulated as

$$f_{E1}^{\mathrm{XRMS}} = \frac{3}{4|\mathbf{k}|}[(\hat{\epsilon}' \cdot \hat{\epsilon})F^{(0)} - \imath(\hat{\epsilon}' \times \hat{\epsilon}) \cdot \hat{\mathbf{z}}_\mathbf{n} F^{(1)} + (\hat{\epsilon}' \cdot \hat{\mathbf{z}}_\mathbf{n})(\hat{\epsilon} \cdot \hat{\mathbf{z}}_\mathbf{n})F^{(2)}], \quad (1)$$

where $\hat{\epsilon}$ and $\hat{\epsilon}'$ are the incident and scattered polarization vectors, $\mathbf{k}$ is the incident x-ray wave vector, and $\hat{\mathbf{z}}_\mathbf{n}$ is a unit vector in the direction of the magnetic moment of the nth ion. The first term in the XRMS amplitude simply contributes to the charge Bragg peak. The second term involves a rank 1 tensor with odd time-reversal symmetry arising from a net spin polarization of the $4f$ states, producing the first-order magnetic satellites. The third term contains a rank 2 tensor with even time-reversal symmetry and includes two powers of the magnetic moment, producing second-harmonic magnetic satellites. By resolving the x-ray wave vectors and magnetic moment vectors into the diffraction plane coordinate system components $\hat{\mathbf{u}}_1$, $\hat{\mathbf{u}}_2$, and $\hat{\mathbf{u}}_3$ (see Fig. 6) of Blume and Gibbs,[21] Hill and McMorrow rewrote Eq. (1) as 2×2 matrices using the polarization states σ and π as basis states, showing the polarization dependence of the XRMS amplitude:[22]

$$f_{E1}^{\mathrm{XRMS}} = F^{(0)}\begin{pmatrix} 1 & 0 \\ 0 & \cos 2\theta \end{pmatrix} - \imath F^{(1)}\begin{pmatrix} 0 & z_1 \cos\theta + z_3 \sin\theta \\ z_3 \sin\theta - z_1 \cos\theta & -z_2 \sin 2\theta \end{pmatrix} + F^{(2)} \times \begin{pmatrix} z_2^2 & -z_2(z_1 \sin\theta - z_3 \cos\theta) \\ z_2(z_1 \sin\theta + z_3 \cos\theta) & -\cos^2\theta(z_1^2 \tan^2\theta + z_3^2) \end{pmatrix}, \quad (2)$$

where θ is the Bragg angle. Hill and McMorrow also gave the $E2$ electric quadrupole XRMS amplitude in their paper.[22]

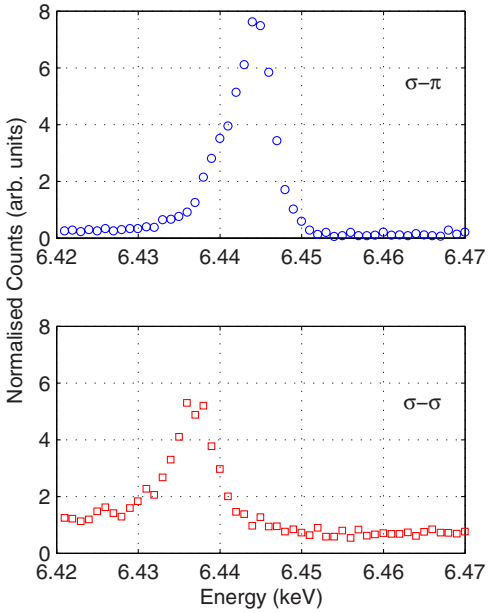

FIG. 7. (Color online) Energy dependence of the $(\frac{1}{2},\frac{5}{4},\frac{5}{4})$ magnetic reflection in PrB_6 in both scattering channels at $T=1.8$ K and $\Psi=-75°$, showing a dipolar resonance ($E1$) in $\sigma-\pi$ and quadrupolar resonance ($E2$) in $\sigma-\sigma$.

As shown in Eq. (2), the XRMS amplitude is anisotropic and depends on the orientation of the magnetic moment. This anisotropy is observed through the variation in the scattered intensity upon rotation of the sample about the scattering vector through the azimuth angle Ψ, defined relative to a reference vector in our case [001]. Therefore, by measuring the azimuthal dependence of the scattered intensity, the magnetic structure may be determined.

1. Commensurate magnetic satellites

Satellite reflections were observed at $T=1.8$ K at the commensurate positions $(\frac{1}{2},\frac{5}{4},\frac{5}{4})$, $(\frac{1}{2},\frac{7}{4},\frac{7}{4})$, and $(\frac{3}{2},\frac{7}{4},\frac{7}{4})$, corresponding to the $(\frac{1}{2},\frac{1}{4},\frac{1}{4})$ ordering wave vector. Energy scans showed resonances in both the $\sigma-\pi$ and $\sigma-\sigma$ channels. As shown in Fig. 7, for $(\frac{1}{2},\frac{5}{4},\frac{5}{4})$ at $\Psi=-75°$ the $\sigma-\pi$ intensity resonates at an incident photon energy of 6.444 keV, identified with the Pr L_{II} $E1$ dipolar transition, whereas there is a 7 eV relative shift for the $\sigma-\sigma$ resonance to 6.437 keV, indicating that this arises from the $E2$ quadrupolar transition. At other azimuthal positions a double peak was seen in energy scans for $\sigma-\sigma$, but the peak at the $E1$ energy was found to be feedthrough from the $\sigma-\pi$ channel due to the imperfect energy match for the Cu (2 2 0) analyzer. The absence of scattering intensity in $\sigma-\sigma$ at the $E1$ energy at all values of Ψ is consistent with a magnetic reflection, as shown by the zero matrix element in the second term in Eq. (2). We exclude the possibility that this peak arises from quadrupolar order since one would then expect scattering in $\sigma-\sigma$ which varied as a function of azimuth. However, it should be noted that such a signal may have been masked by the feedthrough signal from $\sigma-\pi$ due to the imperfect polarization analysis. An investigation of the magnetic scattering cross section for an $E2$ quadrupolar transition, as was given by Hill and McMorrow,[22] shows that it is not immediately apparent why an $E2$ resonance should be seen only in the $\sigma-\sigma$ channel and not in $\sigma-\pi$. Regrettably, due to time constraints, we were unable to determine whether this is the case for all azimuthal angles and further measurements are necessary.

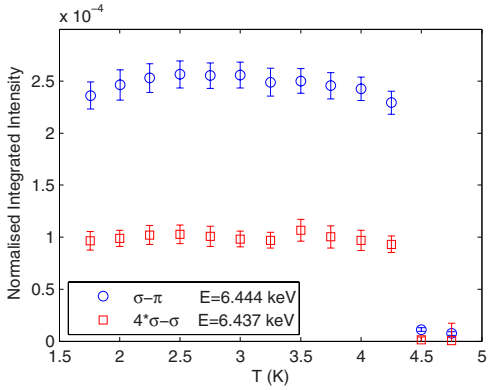

FIG. 8. (Color online) Temperature dependence of the $(\frac{1}{2},\frac{7}{4},\frac{7}{4})$ commensurate magnetic peak in PrB_6 in $\sigma-\pi$ and $\sigma-\sigma$ at their resonant energies. (The intensities of the $\sigma-\sigma$ data have been multiplied by a factor of 4 for ease of viewing.)

The temperature dependence of the $(\frac{1}{2},\frac{7}{4},\frac{7}{4})$ commensurate magnetic peak was measured in both channels at the relevant resonant energies. Figure 8 shows the integrated intensity obtained by fitting a Lorentzian-squared function to each θ rocking curve, normalized to the monitor, for the two channels as a function of temperature. This demonstrates the extremely sharp transition at $T\simeq 4.5$ K above which there is no intensity at this wave vector in reciprocal space.

The azimuthal (Ψ) dependence of the magnetic commensurate peak $(\frac{1}{2},\frac{5}{4},\frac{5}{4})$ was measured in the $\sigma-\pi$ channel at the $E1$ resonance and in the $\sigma-\sigma$ channel at the $E2$ resonance. Figure 9 shows the azimuthal data over a 180° data range. The positions of the maximum and minimum are dictated by

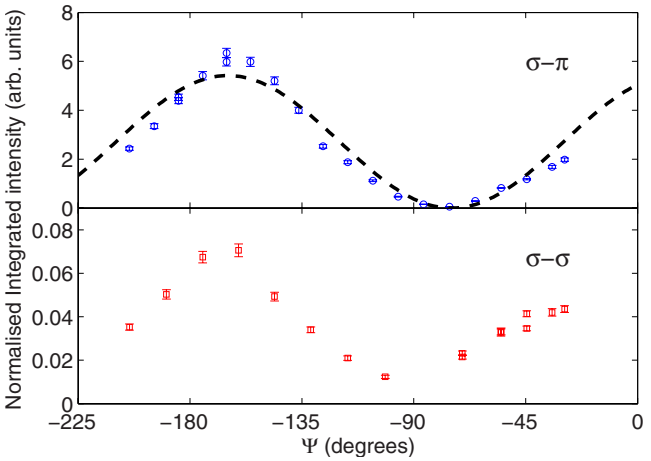

FIG. 9. (Color online) Azimuthal dependence of the scattered intensity from the $(\frac{1}{2},\frac{5}{4},\frac{5}{4})$ commensurate magnetic peak in PrB_6 in the $\sigma-\pi$ channel (○) at the $E1$ resonance and $\sigma-\sigma$ channel (□) at the $E2$ resonance at $T=1.7$ K, with a calculation (–) for $\sigma-\pi$ for the magnetic structure shown in Fig. 1.

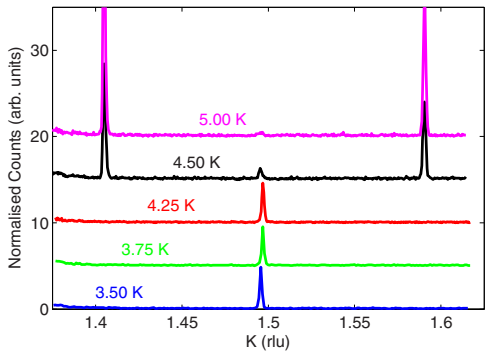

FIG. 10. (Color online) Scans along the reciprocal space K direction across the $(0,\frac{3}{2},\frac{3}{2})$ peak in PrB_6 in the $\sigma-\sigma$ channel at $E=6.444$ keV showing the second-harmonic charge satellites in the commensurate and incommensurate phases and their coexistence at $T=4.5$ K. (The counts from the $T=4.5$ K data have been multiplied by 2 to make it possible to see the commensurate peak, and for ease of comparison each data set has been offset vertically by 5 arbitrary units.)

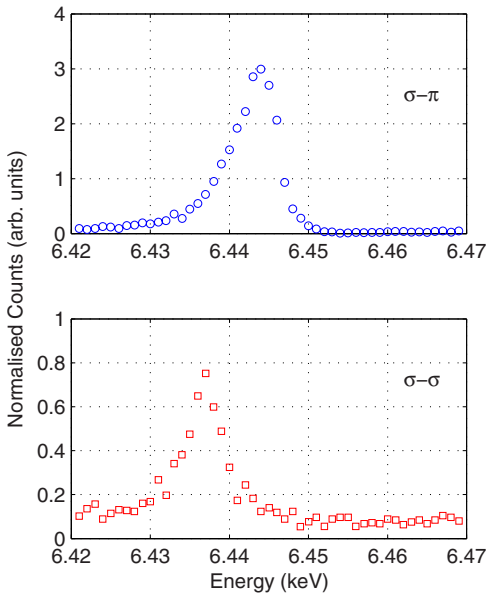

FIG. 11. (Color online) The energy dependence of the incommensurate magnetic satellite at $(\frac{1}{2},\frac{7}{4}+\delta,\frac{7}{4})$ in both scattering channels at $T=5$ K.

the magnetic structure and our zero reference vector [001]. Inspection of Fig. 9 reveals that the positions of the minima differ for the two different resonances. A neutron-diffraction study[8] has proposed the planar double-k magnetic structure for the commensurate phase shown in Fig. 1(a). By evaluating the phase factor weighted sum of the magnetic moments on the Pr ions comprising the magnetic unit cell to give a magnetic structure factor f, the azimuthal dependence of $(\hat{\boldsymbol{\epsilon}}'\times\hat{\boldsymbol{\epsilon}})\cdot f$ for this structure may be calculated. The result is shown as the dashed line in Fig. 9 and is in very good agreement with the measured $\sigma-\pi$ data. Since the calculation was based on the high-temperature cubic crystal structure, the good agreement with the data suggests that the distortion from a cubic structure at the commensurate-incommensurate transition is not very large, consistent with the observation of a distortion of $\leq 0.3\%$ detailed in Sec. III A.[23] It is more problematic to model the $\sigma-\sigma$ data since there is interference between $E1$ and $E2$, and the imperfect analyzer energy led to some feedthrough from $\sigma-\pi$ into $\sigma-\sigma$. It will be important to determine whether there is zero signal in $\sigma-\pi$ at $E2$ for all values of the azimuth, as this will enable us to deduce more about the significance of the $E2$ resonance.

We observed second-harmonic satellites at $2k$ in $\sigma-\sigma$ in the commensurate phase. Since their intensity is predominantly in the $\sigma-\sigma$ channel, and the energy dependence in $\sigma-\sigma$ shows a suppression of $\sim 50\%$ at the Pr L_{II} edge, we identify these as arising from *charge order* rather than magnetic order. The propagation vector of these satellites $(0,\frac{1}{2},\frac{1}{2})$ is reminiscent of that determined to be a secondary lattice distortion associated with the antiferromagnetic order in isostructural GdB_6.[24] Figure 10 shows scans along the reciprocal space k direction through the $(0,\frac{3}{2},\frac{3}{2})$ peak in $\sigma-\sigma$. With increasing temperature, the peak position and intensity remain constant within the commensurate phase. The intensity then drops precipitously at 4.5 K, when incommensurate satellites are observed at $(0,\frac{3}{2}\pm 2\delta,\frac{3}{2})$, where $2\delta\approx 0.1$ rlu. Above 4.5 K there is no intensity at $(0,\frac{3}{2},\frac{3}{2})$.

In GdB_6 an additional lattice modulation was observed with propagation vector $(\frac{1}{2},0,0)$. However, in contrast, a systematic search of PrB_6 reciprocal space failed to observe any scattered intensity at $T=1.7$ K associated with such a modulation. It has been inferred from indirect measurements, and by analogy with CeB_6, that the commensurate magnetic structure is stabilized by quadrupolar order in this phase.[8,11] Also the observation of the crystallographic distortion that appears to be associated with the commensurate-incommensurate phase transition has been predicted to be driven by a quadrupolar transition.[9] The antiferroquadrupolar propagation vector for CeB_6 is reported to be $(\frac{1}{2},\frac{1}{2},\frac{1}{2})$.[13] We have found an analogous superlattice peak in PrB_6 at $(\frac{1}{2},\frac{3}{2},\frac{3}{2})$ with scattering in $\sigma-\sigma$ but not in $\sigma-\pi$ at an azimuthal angle of $\Psi=-37°$. This is consistent with calculations for antiferroquadrupolar $\mathcal{O}_{xy}$ ordering but could also be indicative of the Thomson scattering from a lattice distortion induced by the quadrupolar order. It is important to note that these measurements were performed at the $E1$ resonance energy, such that we were probing the $5d$ electrons rather than the $4f$ electrons which would give rise to the proposed electric quadrupole moments. While for magnetic order the $5d$ electrons are polarized by the magnetic ordering of the $4f$ electrons, allowing the magnetic structure to be inferred, this is not necessarily the case for quadrupolar order. Therefore measurements made at the $E1$ dipole transition energy are not an unambiguous or direct observation of quadrupolar order in $4f$ systems.[25] We plan further measurements to investigate the temperature and azimuthal dependences of this superlattice reflection, at the $E2$ transition energy, for a direct observation of the ordering of the $4f$ quadrupole moments.

2. Incommensurate magnetic satellites

An incommensurate magnetic satellite reflection was observed at $(\frac{1}{2},\frac{7}{4}+\delta,\frac{7}{4})$, where $\delta\approx 0.05$ rlu, in both channels at the relevant resonant energies (see Fig. 11). As shown in Fig.

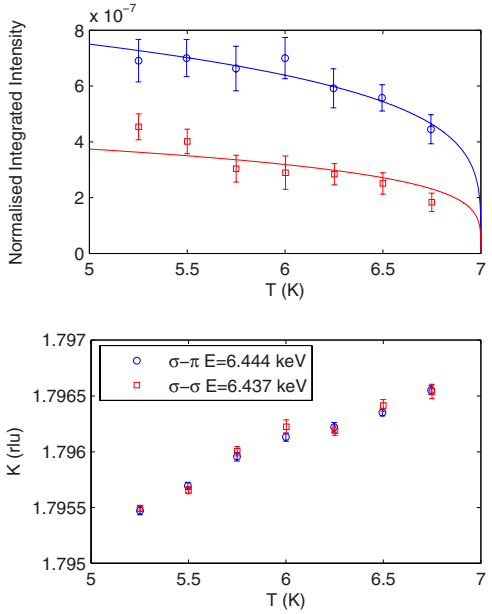

FIG. 12. (Color online) The temperature dependence of (a) the integrated intensity and (b) the center in k of the $(\frac{1}{2},\frac{7}{4}+\delta,\frac{7}{4})$ magnetic peak in PrB_6 in $\sigma-\pi$ and $\sigma-\sigma$ at their resonant energies. The lines in (a) are a guide to the eyes. The signal intensity is zero at $T=7$ K.

12, for $5<T<7$ K the incommensurate peak intensity decreases to zero, while the value of δ increases monotonically by less than 0.1% over this temperature range. Initial measurements of the azimuthal dependence of the intensity of this reflection, performed at $T=5.25$ K in $\sigma-\pi$ at $E1$ and $\sigma-\sigma$ at $E2$, yield results qualitatively similar to those in the commensurate phase.

Second-harmonic incommensurate satellites were observed at $(0,\frac{3}{2}\pm 2\delta,\frac{3}{2})$ in the phase $4.5<T<7$ K in $\sigma-\sigma$. These were again identified as being due to charge ordering (cf. peaks at $(0,\frac{3}{2},\frac{3}{2})$ in the C phase). At $T\sim 4.5$ K there is a mixed phase with peaks observed at both the commensurate and incommensurate reflections as seen in Fig. 10 demonstrating a hysteretic behavior. In the incommensurate phase the peaks decrease in intensity gradually reducing to zero as the temperature is raised into the paramagnetic phase (see Fig. 13).

IV. CONCLUSIONS

In conclusion, using x-ray resonant scattering techniques, we have observed the previously proposed structural distortion and demonstrated that it is associated with the commensurate-incommensurate magnetic transition. The precise details of the distortion cannot be determined from these measurements, and an answer as to its nature will have to await the results from high-resolution neutron powder diffraction. The distortion may be driven by an ordering of the Pr $4f$ quadrupole moments, and we have observed evidence of a reflection not inconsistent with long-range quadrupolar order. Further beam time is required to investigate the $(\frac{1}{2},\frac{3}{2},\frac{3}{2})$ superlattice reflection at the $E2$ resonance energy to determine unambiguously whether this scattering is associated with quadrupolar order.

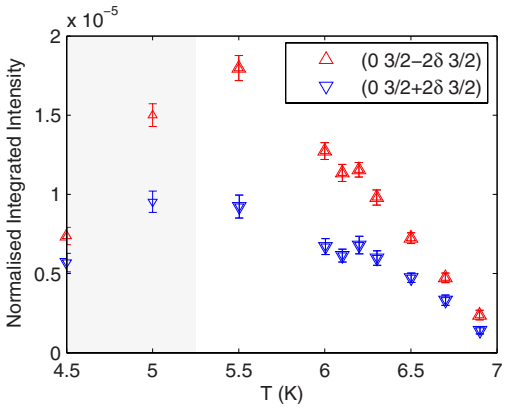

FIG. 13. (Color online) Temperature dependence of the integrated scattered intensity from the incommensurate charge satellites $(0,\frac{3}{2}\pm 2\delta,\frac{3}{2})$ of PrB_6 in $\sigma-\sigma$. The shaded region indicates the temperature range of the mixed commensurate-incommensurate phase.

Magnetic reflections have been identified in the commensurate and incommensurate phases at $(h+\frac{1}{2},k\pm(\frac{1}{4}+\delta),l\pm\frac{1}{4})$ for $\delta=0$ and ~ 0.05, respectively. These reflections display resonant behavior in both polarization channels, and further experiments are planned to explore the origin of the unrotated $E2$ resonance. The azimuthal dependence of the scattered intensity in the commensurate magnetic phase is in agreement with a model for the magnetic structure deduced from neutron-diffraction studies and is little different from that in the incommensurate phase.

ACKNOWLEDGMENTS

The authors thank Paul Thompson for all his help, particularly with the magnet. H.C.W. thanks the Engineering and Physical Sciences Research Council for the provision of a research studentship. Work at Sungkyunkwan University was supported by the KOSEF through the Acceleration Research Program (Grant No. R17-2008-033-01000-0) and the CNRF project.

*k.mcewen@ucl.ac.uk

†Present address: Department of Physics and Astronomy, Rutgers, The State University of New Jersey, 136 Frelinghuysen Road, Piscataway, NJ 08854-8019 USA.

‡Present address: Institut Néel, 25 avenue des Martyrs, Bâtiment E, BP 166, 38042 Grenoble cedex 9, France.

[1] E. E. Vanstein, S. M. Blokhin, and Y. B. Paderno, Sov. Phys. Solid State **6**, 281 (1965).

[2] P. A. Alekseev, J.-M. Mignot, J. Rossat-Mignod, V. N. Lazukov, I. P. Sadikov, E. S. Konovalova, and Y. B. Paderno, J. Phys.: Condens. Matter **7**, 289 (1995).
[3] P. S. Riseborough, Phys. Rev. B **68**, 235213 (2003).
[4] F. Yakhou, V. Plakhty, H. Suzukic, S. Gavrilov, P. Burlet, L. Paolasini, C. Vettier, and S. Kunii, Phys. Lett. A **285**, 191 (2001).
[5] H. Nakao, K. Magishi, Y. Wakabayashi, Y. Murakami, K. Koyama, K. Hirota, Y. Endoh, and S. Kunii, J. Phys. Soc. Jpn. **70**, 1857 (2001).
[6] A. Takase, K. Kojima, T. Komatsubara, and T. Kasuya, Solid State Commun. **36**, 461 (1980).
[7] T. H. Geballe, B. T. Matthias, K. Andres, J. P. Maita, A. S. Cooper, and E. Corenzwit, Science **160**, 1443 (1968).
[8] P. Burlet, J. M. Effantin, J. Rossat-Mignod, S. Kunii, and T. Kasuya, J. Phys. (Paris) **49**, C8 (1988).
[9] C. M. McCarthy, C. W. Tompson, R. J. Graves, H. W. White, Z. Fisk, and H. R. Ott, Solid State Commun. **36**, 861 (1980).
[10] M. Loewenhaupt and M. Prager, Z. Phys. B: Condens. Matter **62**, 195 (1986).
[11] S. Kobayashi, M. Sera, M. Hiroi, T. Nishizaki, N. Kobayashi, and S. Kunii, J. Phys. Soc. Jpn. **70**, 1721 (2001).
[12] M. D. Le, K. A. McEwen, J.-G. Park, S. Lee, F. Iga, and K. C. Rule, J. Phys.: Condens. Matter **20**, 104231 (2008).
[13] J. M. Effantin, J. Rossat-Mignod, P. Burlet, H. Bartholin, S. Kunii, and T. Kasuya, J. Magn. Magn. Mater. **47-48**, 145 (1985).
[14] S. Awaji, N. Kobayashi, S. Sakatsume, S. Kunii, and M. Sera, J. Phys. Soc. Jpn. **68**, 2518 (1999).
[15] S. D. Brown *et al.*, J. Synchrotron Radiat. **8**, 1172 (2001).
[16] A. Gibaud, T. W. Ryan, and R. J. Nelmes, J. Phys. C **20**, 3833 (1987).
[17] J.-G. Park, S. Lee, *et al.* (unpublished).
[18] H. C. Walker, K. A. McEwen, D. F. McMorrow, S. B. Wilkins, F. Wastin, E. Colineau, and D. Fort, Phys. Rev. Lett. **97**, 137203 (2006).
[19] K. A. McEwen, H. C. Walker, M. D. Le, D. F. McMorrow, E. Colineau, F. Wastin, S. B. Wilkins, J.-G. Park, R. I. Bewley, and D. Fort, J. Magn. Magn. Mater. **310**, 718 (2007).
[20] T. Matsumura, N. Oumi, K. Hirota, H. Nakao, Y. Murakami, Y. Wakabayashi, T. Arima, S. Ishihara, and Y. Endoh, Phys. Rev. B **65**, 094420 (2002).
[21] M. Blume and D. Gibbs, Phys. Rev. B **37**, 1779 (1988).
[22] J. P. Hill and D. F. McMorrow, Acta Crystallogr., Sect. A: Found. Crystallogr. **52**, 236 (1996).
[23] Detailed calculations show that the azimuthal dependence is not sensitive to distortions of $\leq 1\%$ within the error bars of the experiment.
[24] D. F. McMorrow, K. A. McEwen, J.-G. Park, S. Lee, D. Mannix, F. Iga, and T. Takabatake, Physica B **345**, 66 (2004).
[25] Y. Tanaka *et al.*, Phys. Rev. B **69**, 024417 (2004).